Naunyn-Schmiedeberg's Archives of Pharmacology (2019) 392:1465–1476
https://doi.org/10.1007/s00210-019-01688-1

ORIGINAL ARTICLE

In vitro study of the cytotoxicity of thymoquinone/curcumin fluorescent liposomes

Heba Mohamed Fahmy[1]

Received: 9 March 2019 / Accepted: 28 June 2019 / Published online: 3 August 2019

Abstract

In the present study, thymoquinone-loaded liposomes (Lip (TQ)), curcumin-encapsulated liposome (Lip (CUR)), and thymoquinone/curcumin-encapsulated liposome (Lip (TQ + CUR)) in addition to rhodamine-labeled thymoquinone/curcumin liposome (Lip (TQ + CUR + ROD)) were prepared with encapsulation efficiency exceeding 99%. The aim of the present study was to evaluate the effect of the different prepared formulations either labeled with the fluorescent dye (rhodamine B) or not on A549 lung cancer cells. Cytotoxicity of different formulations was assessed by MTT assay. Proliferation of A549 cells was significantly inhibited by the different formulations in a concentration-dependent manner in 72 h. The Lip (TQ + CUR + ROD) formulation demonstrated the lowest IC_{50} value. To investigate its mechanism of action on A549 lung cancer cells, the Comet assay (for DNA damage) was done, the measurement of some oxidative stress parameters in addition to performing inverted fluorescence microscopy imaging. The results of the present study demonstrated the increased DNA damage, oxidative stress damage, and cell apoptosis in A549 treated with TQ, CUR, and rhodamine-encapsulated fluorescent liposome formulation as compared to untreated cells. The results obtained from the present study demonstrate the significant role of the TQ/CUR fluorescent liposomes on decreasing the viability of A549 lung cancer cells.

Keywords Thymoquinone · Curcumin · Rhodamine B · Liposome · Fluorescent microscope · Comet assay

Introduction

Thymoquinone (TQ) which is the bioactive compound of *Nigella sativa* demonstrated strong suppression of the proliferation of various tumor cells (Worthen et al. 1998). TQ inhibits cell proliferation, decreases cellular viability, induces apoptosis, and arrests cell cycle; in addition, it has been demonstrated that it acts on multiple molecular targets (Randhawa and Alghamdi 2011). Nevertheless, its use is limited due to its poor water solubility (Gali-Muhtasib et al. 2006). In sum, it was reported that administration of large dosages of TQ to rats led to liver and kidney toxicity (Badary et al. 1998). In a previous study, lung cancer cells were treated with various concentrations of TQ for different periods of time. The results showed that TQ played a role in inhibiting proliferation, invasion, and migration of A549 lung cancer cells and it inhibited the expression level of PCNA, cyclin D1, MMP2, and MMP9 mRNA and protein in a dose- and time-dependent manner (Yang et al. 2015).

Curcumin is a lipophilic molecule and passes easily through the plasma membrane into the cytosol (Oetari et al. 1996). Curcumin can inhibit cell proliferation and inflammation, induce apoptosis, and sensitize tumor cells (Karunagaran et al. 2005; Thangapazham et al. 2006; Srivastava et al. 2007). Lin et al. (2009) studied the effects of anti-tumor invasion and migration of A549 lung cancer cells. The results indicated that curcumin had anti-metastatic potential by reducing cancer cell invasiveness. Likewise, the author suggested that curcumin had anti-cancer effect of the suppression of migration and invasion in A549 lung cancer cells. Nevertheless, it is well known that curcumin is poorly taken up in the blood (Chauhan 2002); thus, further studies should as well be concentrated on increasing the bioavailability of curcumin (Chauhan 2002).

Liposomes are composed of single or multiple concentric lipid bilayers encapsulating an aqueous compartment (Bangham et al. 1974). Liposomes seem to be an ideal system of drug-carrying in vivo and in vitro, since their morphology is identical to that of cellular membranes and due to their ability to incorporate various substances. They have biological and

✉ Heba Mohamed Fahmy
heba_moh_fahmi@yahoo.com

[1] Biophysics Department, Faculty of Science, Cairo University, 16 El Zafer Street, Haram, Giza, Egypt

technological advantages as an optimal delivery system for biologically active substances (Felice et al. 2014). Drugs encapsulated in liposomes are not bioavailable until they are released (Bozzuto and Molinari 2015). Treatments with liposomes proved to improve patient outcome, decreasing some of the side effects associated with chemotherapy when compared to unencapsulated drugs (Lasic 1998; Zamboni 2008). It has been shown that the activity of liposomal curcumin was similar or better than that of free curcumin at equimolar concentrations (Kurzrock and Li 2005). Liposomes are excellent to act as solubilizing agent and drug carrier for TQ to enhance its bioavailability and its uptake by cells (Ravindran et al. 2010).

Previous studies proved that curcumin as well as thymoquinone may have effects on the development or progression of cancer (in vitro). Curcumin, alone or in combination, shows chemopreventive and anti-cancer activities against various cancer types with reported uses (Wong et al. 2019), including colorectal (Shehzad et al. 2013), pancreatic (Ma et al. 2014), head and neck (Wilken et al. 2011), breast (Li et al. 2014), prostate (Guo et al. 2013), lung (Jin et al. 2015), and oral cancers (Zhen et al. 2014). Thymoquinone is obvious as a powerful molecule against cancer by controlling various molecular processes and can be a useful tiny therapeutic molecule in cancer prevention and therapy (Khan et al. 2017). Majdalawieh et al. (2017) concluded that TQ is a potent therapeutic agent for the suppression, growth, and metastasis of tumor development in a spectrum of tumors. Dehghani et al. (2015) found that thymoquinone and nanothymoquinone considerably inhibited the proliferation of MCF7 cells in a concentration-dependent manner.

The aim of the present work was to prepare and characterize thymoquinone/curcumin liposomes and to evaluate their anti-cancer effect on the A549 lung cancer cells. The aim of the present study extends also to study the mechanism of cytotoxicity of thymoquinone/curcumin liposomes labeled with rhodamine B on the A549 lung cancer cells.

Materials and methods

Chemicals used

1,2-dipalmitoyl-Sn-glycero-3-phosphocholine (DPPC), chloroform solution (HPLC grade), phosphate-buffered saline (PBS), curcumin, thymoquinone, and rhodamine B were purchased from Sigma-Aldrich and were used without any further purification. Figure 1 shows the chemical structure of both thymoquinone and curcumin.

Preparation of liposomes

Five types of liposomes were prepared: DPPC liposomes (Lip), thymoquinone-loaded liposomes (Lip (TQ)), curcumin-loaded liposomes (Lip (CUR)), thymoquinone/curcumin-loaded liposomes (Lip (TQ + CUR)), and fluorescent thymoquinone/curcumin-loaded liposomes (Lip (TQ + CUR + ROD)). Liposomes were prepared using the thin film hydration method as previously described by Bangham et al. (1974). Briefly, 10 mg of DPPC was weighted and dissolved in 3 ml chloroform in a 250-ml round bottom flask, and then, 7 mg of thymoquinone was added to them. The chloroform was then evaporated under nitrogen stream vacuum using hand shaking maintained in a 50 °C water bath (ATK 250, AHAAM) until a thin dry film of lipid was formed along the walls of the flask. After that, the thin lipid film was hydrated by adding 5 ml saline buffer phosphate-buffered saline (PBS) (pH 7) and left for 24 h at room temperature for complete hydration. Lip (CUR), Lip (TQ), Lip (CUR + TQ), and Lip (CUR+ TQ+ ROD) liposomes were prepared utilizing the same method described above, but by adding 7 mg of curcumin, 7 mg of thymoquinone (7 mg of thymoquinone + 7 mg of curcumin) and (7 mg of curcumin + 7 mg of thymoquinone + 1 mg rhodamine B), respectively. The size of prepared liposomes was controlled using both vortex and sonication techniques. The liposome dispersion was vortexed for about 2–3 min and then sonicated in an ultrasonic bath sonicator (MCS, Digital ultrasonic cleaner, model CD-4820) for approximately 3–5 min.

Characterization of the prepared liposomes

Differential scanning calorimetry

Thermal analysis was carried out using a differential scanning calorimeter (DSC-60 Shimadzu). The samples were placed in hermetically sealed standard aluminum differential scanning calorimetry (DSC) pans and scanned over a temperature range of 0–100 °C at a heating rate of 5 °C min^{-1}. An empty pan was used as a reference to eliminate the calorimetric effect of the pan.

Dynamic light scattering

By dynamic light scattering (DLS) technique using the Malvern Zeta Sizer model 1000HSa, the hydrodynamic diameter of DPPC liposomes was determined. The instrument calculates the average size of the liposomes depending on the measured time-dependent fluctuations of the light scattered by liposomes.

Zeta potential analysis

Using Zetasizer Nano ZS90 (Malvern Instruments, UK), the zeta potentials and electrophoretic mobilities of liposomes were measured. The liposomes solution was placed in the sample holder and a laser beam at 633 nm was localized on the sample. Scattered light was detected by a photomultiplier tube.

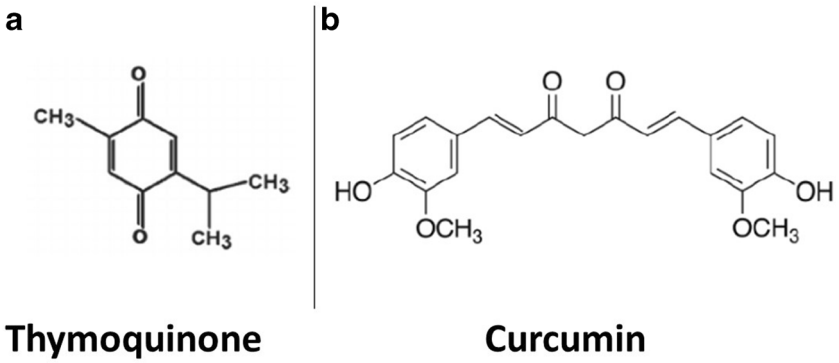

Fig. 1 The chemical structure of a thymoquinone and b curcumin

Transmission electron microscopy

Transmission electron microscopy (TEM) imaging was used to examine the morphology and the structure of liposome vesicles. A drop of diluted vesicles was applied to a copper-coated grid and left to dry for15 min. Excess dispersion was removed with a piece of filter paper. The samples were negatively stained using one drop of 1% phosphotungstic acid, left in the breeze for about 1 s then examined with high-resolution transmission electron microscope TEM (Jeol-2100).

Fourier transform infrared spectroscopy

Infrared spectra were measured using a (4100 Jasco-Japan) Fourier transform infrared spectroscopy (FTIR) spectrometer. The instrument was under continuous dry air purge to eliminate atmospheric water vapor. Through this technique, it is possible to monitor fine changes in the structure of the lipid assemblies by analyzing the frequency and the bandwidth variations of the vibrational modes.

Encapsulation efficiency measurements

The encapsulation efficiency (EE%) was calculated for Lip (CUR), Lip (TQ), Lip (CUR + TQ), and lip (CUR+ TQ+ ROD). The four samples were centrifuged at 8500 rpm (VS-18000M, Korea, power 220 V/50 HZ) for 30 min, to separate the free drug (supernatant) from the encapsulated one (pellet). The clear supernatant was then collected and vortexed to obtain a homogeneous mixture, while the pellets obtained after centrifugation were diluted with 10 ml saline buffer (Ph 7) and were sonicated for 10 min for further use. This procedure was duplicated three times for each sample. The absorbance of curcumin was measured at different concentrations using a UV-visible spectrophotometer (JENWAY 6405, UK) at 558 nm (the resonance absorption of curcumin). The calibration curve of curcumin was made by plotting the absorbance against the immersion. The absorbance of the free curcumin in the supernatant was determined spectrophotometrically at 558 nm. The same steps were repeated for the free drug obtained from the samples: Lip (TQ), Lip (TQ + CUR), and Lip (TQ + CUR + ROD) by adjusting the spectrophotometer wavelength at 265 nm for thymoquinone, 558 nm for curcumin, and 547 nm for rhodamine B. The concentration of the free drug in the supernatant was calculated from the calibration curve made for both the curcumin and thymoquinone separately and the encapsulation efficiency for both was calculated from the following equation:

$$\text{Encapsulation efficiency}\% = \frac{\text{Initial conc} - \text{final conc}}{\text{Initial conc}} \times 100\ \%.$$

Cell culture

Human lung carcinoma cell lines A549 was purchased from VACSERA research foundation Egypt. Cells were cultured in 75-cm^2 cell culture flasks with 10% FBS as a culture medium, 1% penicillin–streptomycin, and 1% glutamine and grown at 37 °C under conditions of humidified 5% CO2 and 95% air at one atmosphere.

Cell viability assay

Cell viability was assessed by MTT (3,4,5-dimethyl-thiazol-2-yl)-2-5-diphenyltetrazolium bromide) assay, which depended on MTT reduction by the mitochondrial dehydrogenase of intact cells in the output of a purple formazan (Farrow and Brown 1996; Goel et al. 2001). Cells were plated in each wall of a 96-well plates. Cells were placed in the humidified 5% CO_2 incubator at 37 °C allowing for attachment to the substratum from 2 to 3 days and placed in the humidified 5% CO2 incubator for 2 h. The cells incubated in culture medium alone served as a control for cell viability. The cell viability assay was performed for all the liposome formulations in addition to thymoquinone, curcumin, and rhodamine B in their free forms to assess the IC50 for all the tested formulations.

Comet assay

Cells were counted and aliquots of 100 μL of the cell suspension were set on each wall of 96-well plates, treated with

100 μl aliquots of media, and incubated in a 5% CO_2 at 37 °C for 2 h. Upon incubation, the cells were centrifuged, washed with PBS free calcium and magnesium, and re-suspended in the 100 μL PBS. In a 2-ml tube, 50 μL of the cell suspension and 500 μL of melted LM Agarose were mixed and 75 μL was pipetted onto a pre-warmed comet slide. The side of the pipette tip was used for spreading completely agarose/cells over the sample area. The slides were placed flat in the dark at 4 °C for 10 min to allow the mixture to solidify and then immersed in a prechilled lysis solution at 4 °C for 40 min. The slides were removed from lysis solution, tapped and immersed in alkaline solution for 40 min at room temperature in the dark. The slides were washed twice for 5 min with Tris-Borate-EDTA (TBE). The slides were electrophoresed at low voltage for 20 min. The slides were located in 70% ethanol for 5 min, removed, tapped, and air-dried for overnight. The slides were stained with SYBR green stain designed for the comet assay and set aside to air dry at room temperature for 6 h. SYBR Green stained comet slides were viewed with an Olympus fluorescence microscope and analyzed using LAI's Comet assay analysis system software.

Inverted fluorescence microscope

Both untreated A549 cells and A549 cells treated with TQ, CUR, and rhodamine B-encapsulated liposome were screened using LEICA DMI 4000 B inverted fluorescence microscope.

Determination of oxidative stress parameters in A549 lung cancer cell lines

Determination of lipid peroxidation levels

Lipid peroxidation was assayed by measuring the levels of thiobarbituric reactive species using the method of Ruiz-Larrea et al. (1994), in which the thiobarbituric acid reactive substances react with thiobarbituric acid to produce a pink colored complex whose absorbance is read at 532 nm in a Helios Alpha Thermospectronic (UVA 111615, England).

Determination of glutathione levels

Measurement of reduced glutathione levels was carried out spectrophotometrically using Beutler et al. (1963) method. It relies on the reduction of 5,5′-dithiobis 2-nitrobenzoic acid (DTNB) with glutathione to produce a yellow color. The absorbance of the reduced chromogen is measured at 405 nm in a Helios alpha thermospectronic (UVA 111615, England).

Determination of superoxide dismutase activity

Superoxide dismutase (SOD) activity was determined according to the method of Nishikimi et al. (1972). The assay for SOD levels was performed using Biodiagnostic kit No. SD 25 21. This assay relies on the ability of the enzyme to inhibit the phenazine methosulphate mediated reduction of nitroblue tetrazolium dye.

Results

Effect of encapsulation of DPPC liposome on the ultrastructure

Transmission electron micrographs were taken out for Lip, Lip (TQ), Lip (CUR), Lip (TQ + CUR), and Lip (TQ + CUR + ROD) as shown in Fig. 2. TEM images demonstrated the presence of regular and relatively homogeneous multilamellar vesicles (MLVs, with several lamellar phase lipid bilayers). The morphology of all liposomes is nearly spherical in shape with large internal aqueous core and few aggregations.

Effect of encapsulation of DPPC liposome on DSC charts

As seen in Fig. 3, the main phase transition peaks of Lip were found at: 43.51 and 50.61 °C, whereas the main phase transition peaks of Lip (TQ) were located at 42.54 and 55.39 °C. Regarding Lip (CUR), 3 endothermic peaks were noted at 39.37, 49.20, and 50.96 °C, respectively. The main phase transition peaks of Lip (TQ + CUR) were noted at 33.02 (a sharp peak), 49.10, 56.03, and 59.93 °C. Finally, the main phase transition peak of Lip (TQ + CUR + ROD) was found at 16.87 °C.

Effect of encapsulation of DPPC liposome on the DPPC liposomal size

As observed in Fig. 4, using DLS, the measured mean diameters of DPPC free liposome (Lip) were 115 ± 2 nm for 96.6%, whereas 3.4% of particles were having a mean diameter of 1149 ± 15 nm. For Lip (TQ), 100% of particles had mean diameter of about 722.9 ± 12 nm. Regarding Lip (CUR), 98.3% of particles have a mean size of 82.74 ± 7 nm and only 1.7% of particles had a peak at 580.5 ± 5.2 nm. For Lip (TQ + CUR), 97.3% of particles had a mean size of 122.9 ± 3 nm and only 2.7% of particles had a size of 1087 ± 15 nm. Finally, for Lip (TQ + CUR + ROD), 86.2% of particles had a mean diameter of 119.8 ± 2.3 nm and the remaining particles (13.8%) had a size of 692.2 ± 9 nm. All measurements were done three times and data was expressed as mean ± standard error of the mean. PBS was the solvent used for DLS measurements, all formulations were measured at a concentration of 0.01 mol/L.

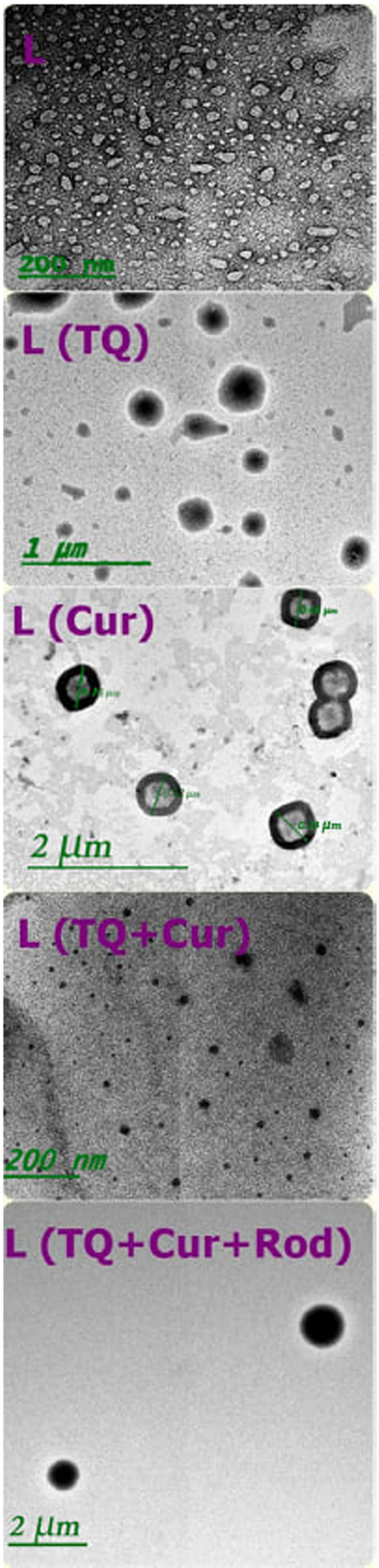

Fig. 2 Effect of encapsulation of DPPC liposome on transmission electron micrographs

Effect of encapsulation of DPPC liposome on the zeta potential

The mean of the zeta potential for free Lip was found to be 5.21 ± 0.5 mV, whereas that for Lip (TQ) was found to be 1.73 ± 0.02 mV. Regarding the Lip (CUR), its zeta potential was found to be − 11 ± 1.1 mV. Going to the Lip (TQ + CUR), its zeta potential recorded − 5 ± 0.2 mV and finally, for Lip (TQ + CUR + ROD), the zeta potential was found to be − 5.71 ± 0.5 mV. All zeta potential measurements were taken in triplicate and the mean ± standard error of the mean was calculated.

The growth inhibitory effect of thymoquinone, curcumin, and rhodamine B on A549 cells at different concentrations

Figure 5 indicates that thymoquinone, curcumin, rhodamine B, thymoquinone + curcumin and thymoquione + curcumin + rhodamine B caused cell death in a dose-dependent manner after a cell incubation period of 72 h in lung cancer cell line A549. The 50% effective dose (ED50) was about 350 μg/ml (2.13 μM), 210 μg/ml (0.57 μM), 415 μg/ml (0.866 μM), 405 μg/ml, and 410 μg/ml for free thymoquinone, curcumin, rhodamine B, thymoquinone + curcumin, and thymoquione + curcumin + rhodamine B in A549 cell line, respectively.

The growth inhibitory effect of encapsulation of DPPC liposome on A549 cells at different concentrations

Figure 6 indicates that Lip, Lip (TQ), Lip (CUR), Lip (TQ + CUR), and Lip (TQ + CUR + ROD) caused cell death in a dose-dependent manner after a cell incubation period of 72 h in lung cancer cell line A549. The half maximal effective concentration was about 335 μg/ml, 315 μg/ml, 270 μg/ml, and 80 μg/ml, 350 μg/ml, 210 μg/ml, 415 μg/ml for Lip (TQ), Lip (CUR), Lip (TQ + CUR), Lip (TQ + CUR + ROD), free TQ, free CUR, and free rhodamine in A549 cell line, respectively (Fig. 7).

The effect of the exposure of A549 lung cancer cells to thymoquinone, curcumin-encapsulated liposome formulation on the oxidative stress status of the cells

As demonstrated in Table 1, the present results show that malondialdehyde (MDA) increased significantly in A549 cells treated with L (TQ + CUR) as compared to untreated A549 cells (P value = 3.7×10^{-5} and % D = 115%). Meanwhile, glutathione (GSH) reported non-significant changes between the two investigated experimental groups (P value = 0.7 and %D = 6.7%). Finally, SOD activity shows a significant increase in A549 cells treated with thymoquinone, curcumin-encapsulated liposome as compared to untreated A549 cells (P value = 0.0018 and %D = 83.94%).

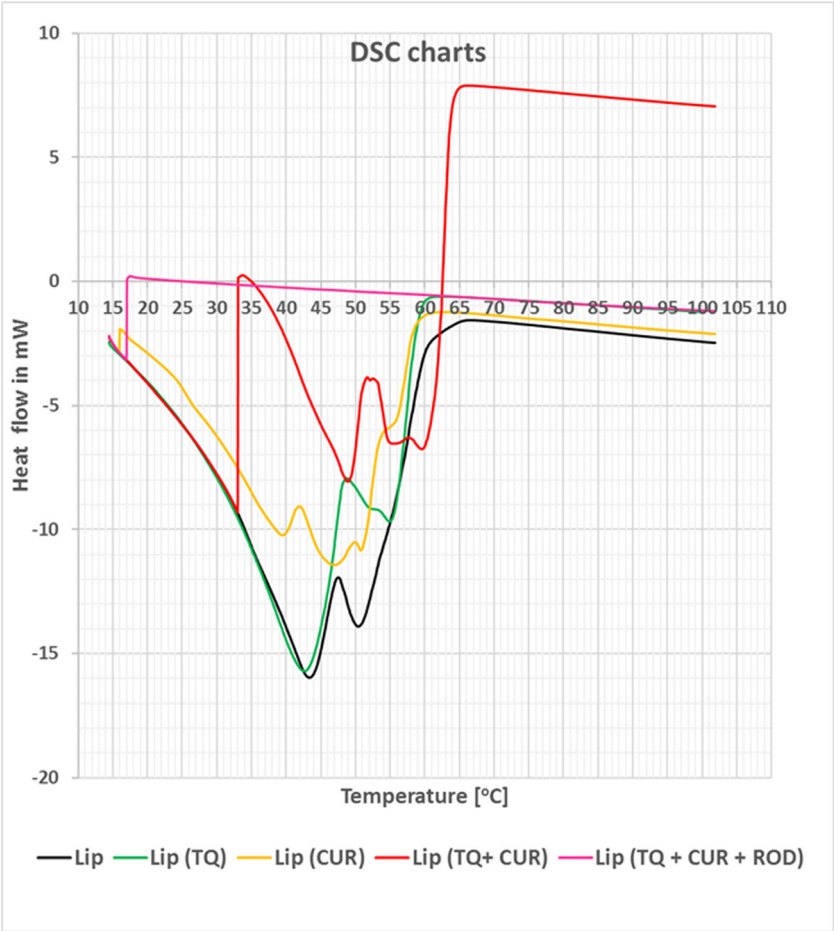

Fig. 3 Effect of encapsulation of DPPC liposome on the DSC charts

The effect of the exposure of A549 lung cancer cells to thymoquinone, curcumin-encapsulated liposome formulation on the DNA of the cells as determined by the comet assay

As seen in Table 2, Figs. 8 and 9, in the present study, the % DNA damage showed a significant increase in A549 cells treated with thymoquinone, curcumin-encapsulated liposome as compared to the untreated A549 lung cells (P value = $1.3e^{-4}$ and %D = 89.21%). In addition, the tail length demonstrated a significant increase in untreated A549 lung cancer cells when compared to A549 cells treated with thymoquinone, curcumin-encapsulated liposome (P value = 0.008 and %D = − 107.73%). It was demonstrated that the percentage DNA in the tail reported non-significant changes between the 2 tested groups (P value = 0.051 and %D =

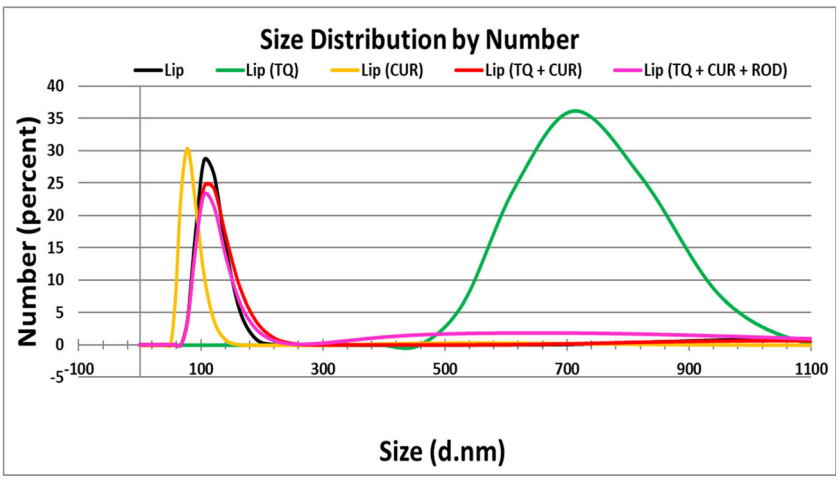

Fig. 4 Effect of encapsulation of DPPC liposome on the DPPC liposome size measured by dynamic light scattering (DLS)

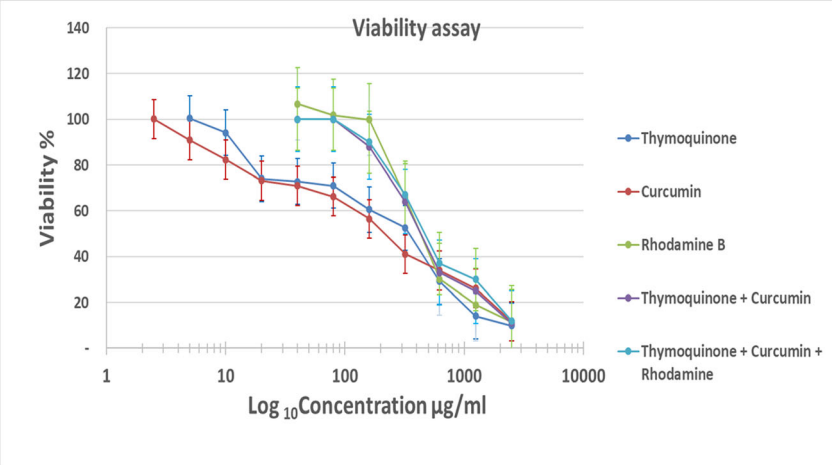

Fig. 5 The growth inhibitory effect of thymoquinone, curcumin, rhodamine B, thymoquinone + curcumin (1:1), and thymoquinone + curcumin + rhodamine B (7:7:1) on A549 cells at different concentrations (2500; 1250, 620, 320, 160, 80, 40, 20, 10, 5, 2.5. Data is expressed as mean ± S.E.M, with $n = 3$). The values were normalized according to the control

23.76%). Meanwhile, the tail moment demonstrated a significant decrease in A549 cells treated with thymoquinone, curcumin-encapsulated liposome as compared to untreated A549 lung cells (P value = 0.002 and %D = − 34.97%).

Morphological changes using inverted fluorescence microscope

Figure 10 shows A549 cells treated with thymoquinone, curcumin, and rhodamine B-encapsulated liposome under inverted fluorescence microscope with most of the cells or their nuclei showed apoptosis. On the other hand, Fig. 11 shows the normal morphology of A549 cancer cells. Most of the cells are viable with spindle or spherical shapes having normal nuclei.

Discussion

The treatment of cancer is a very difficult issue, due to the resistance of cancer to most of the currently used treatment, making cancer treatment, a real challenge. Medicinal plants have been used for several decades for the treatment of a wide range of diseases owning to their availability and low cost.

The present work aimed to develop and characterize (thymoquinone/curcumin) fluorescent liposomes and to evaluate their potential effect on A549 lung cancer cells. Curcumin, one of the major parts of turmeric, the dried rhizome of *Curcuma longa* L., has been demonstrated to possess anti-proliferating and anti-carcinogenic properties. Previous work has indicated that curcumin might affect several cellular processes involved in tumorigenesis and progression (Aggarwal et al. 2013). Thymoquinone (2-isopropyl-5-methyl-1,4-benzoquinone) is an herbal-derived drug with potential chemopreventive and chemotherapeutic activity. However, thymoquinone suffers from high hydrophobicity causing poor solubility, which limits its bioavailability and high lipophilicity causing poor formulation characteristics. In this work, we prepared thymoquinone-encapsulated liposome to enhance its solubility and bioavailability.

Liposomes are versatile drug carriers that can be applied to resolve problems of drug solubility, instability, and bio-distribution. In this study, we were able to prepare thymoquinone-loaded liposomes (Lip (TQ)), curcumin-encapsulated

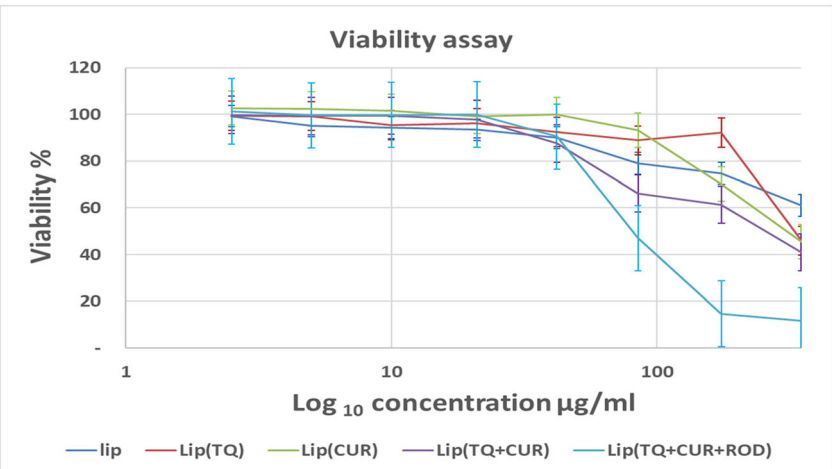

Fig. 6 The growth inhibitory effect of encapsulation of DPPC liposome on A549 cells at different concentrations (350, 175, 85, 42, 21, 10, 5, 2.5 µg/ml). (Data is expressed as mean ± S.E.M, with $n = 3$)

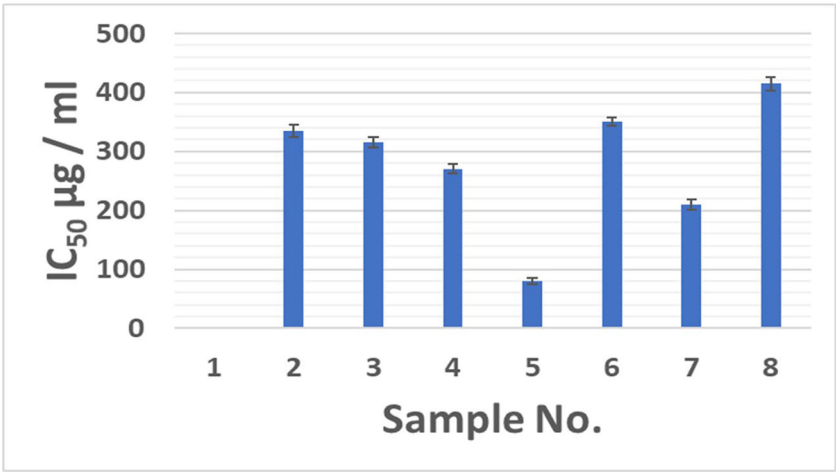

Fig. 7 IC50 values for 1: Lip, 2: Lip (TQ), 3: Lip (CUR), 4: Lip (TQ + CUR), 5: Lip (TQ + CUR + ROD), 6: thymoquinone, 7: curcumin, and 8: rhodamine B (Data is expressed as mean ± S.E.M, with $n = 3$)

liposome (Lip (CUR)), thymoquinone/curcumin-encapsulated liposome (Lip (TQ + CUR)) in addition to rhodamine-labeled thymoquinone/curcumin liposome ((Lip (TQ + CUR + ROD)) with encapsulation efficiency exceeding 99% for all the prepared formulations.

It has been well known from the scientific literature that the zeta potential (ZP) is an important indicator for the stability of liposomal formulations. The ZP is a physical property measured through the electrophoretic mobility of the particles in an electric field (Mishra et al. 2009). It is well accepted that the sign and magnitude of zeta potential are found out by the net charge accumulated on the liposome surface. It was proposed that a minimum ZP value of ± 30 mV is necessary to ensure the stability of a suspension (Jacobs and Müller 2002; Shameli et al. 2012). Harris et al. (2001) suggested that a high absolute value of ZP means a high electric charge on the surface of drug-loaded liposomes, which contribute to strong repulsive force among particles to prevent liposomal aggregation in buffer solutions. It is presently accepted that the higher the value of the ZP, the more stable the suspension, because repulsion occurs between the charged particles to traverse over the innate propensity to aggregate (Heurtault et al. 2003). In the present study, from ZP measurement, it has been indicated that normal unexposed liposomes possess positive surface charges (5.21 mV) which mainly refers to some preferable orientation of the dipoles of polar phospholipid heads. This proposition is further confirmed by the proposition of Makino et al. (1991) who stated that the polar heads of the phospholipid may orient in a different way at the surface, which results in negative, positive, or even zero zeta potential. ZP values of about 20 mV provide only short-term stability, whereas values in the range − 5 to + 5 mV indicate fast aggregations. Encapsulation of DPPC liposomes with thymoquinone resulted in a zeta potential value of 1.73 mv, meaning a loss of repulsive forces between lipids and a high tendency of aggregation. From the particle size results of the thymoquinone-encapsulated DPPC liposomes (722.9 nm), it may be postulated that the encapsulation of thymoquinone in liposomes induces liposome aggregation and finally fusion into larger structure (Svarnas et al. 2012). Previous literature suggested that the negatively charged particles bind at the cationic sites in the form of clusters (Patil et al. 2007).

From the present study, it was found out that the control DPPC liposome sample exhibits 2 main phase transitions at 43.51 and 50.61 °C, respectively. Toyran and Severcan (2002) suggested that the decreases in the phase transition to lower temperature values and the broadening of the phase transition curve implying the loss of cooperativity between the lipid

Table 1 The effect of the exposure of A549 lung cancer cells to L (TQ + CUR) formulation on the oxidative stress status of the cells

Oxidative stress parameter	Untreated A549 cells	A549 cells treated with L (TQ + CUR)		*T* test (*P* value)
		Value	%D	
MDA (mmole/ml)	0.20 ± 0.02 (5)	0.43 ± 0.02 (5)	115%	3.7×10^{-5}*
GSH (mmole/ml)	0.15 ± 0.03 (5)	0.16 ± 0.04 (5)	6.67%	0.77 (n.s.)
SOD activity (U/ml)	170 ± 12.2 (5)	313 ± 28.7 (5)	83.94%	0.0018*

Values represent the mean ± S.E.M. The number of samples is shown between parentheses. *% D*: percentage differences in comparison to untreated cells. %D = (mean of treated cells − mean of untreated cells) / mean of untreated cells

n.s. non-significant; *$p < 0.05$ significant

Table 2 The effect of the exposure of A549 lung cancer cells to L (TQ + CUR) formulation on the DNA of the cells as determined by the comet assay

Comet assay results		
	Untreated A549 cells	A549 cells treated with L (TQ + CUR)
% damage	10.6 ± 0.3 (3)	20 ± 0.6 (3)
	P value = $1.3e^{-4}$ (significant)* %D = 89.21%	
	9.7 ± 1.0 (3)	4.7 ± 0.1 (3)
Tail length	*P* value = 0.008 (significant)* %D = − 107.73%	
Percentage DNA in the tail	13.4 ± 1.4 (3)	17.5 ± 0.6 (3)
	P value = 0.05 (non-significant) %D = 23.76%	
Tail moment	1.4 ± 0.04 (3)	0.9 ± 0.06 (3)
	P value = 0.002 (significant)* %D = − 34.97%	

Values are expressed as mean ± S.E.M. *% D*: percentage differences in comparison to untreated cells. %D = (mean of treated cells − mean of untreated cells) / mean of untreated cells. The number of samples is shown between parentheses

*$P < 0.05$ significant

chains of DPPC. Grounded on this suggestion, it may be evoked that increasing of the second phase transition of DPPC liposomes observed in this study due to the encapsulation of DPPC liposomes with thymoquinone (from 50.61 to 55.39 °C) and also the increasing of the first phase transition in curcumin-encapsulated liposome from (43.51 to 49.20 °C) as compared to free DPPC liposomes can be interpreted as a kind of an increase in the stability (the order) of the lipid chains of DPPC and consequently decreasing its permeability and fluidity. This suggestion is supported too for Lip (CUR) by the results of ZP obtained in the present study, which indicated a tendency to higher stability (increasing ZP to about − 11 mV. Díaz-Visurraga et al. (2012) stated that the exothermic peaks that appear during the DSC recording result from decomposition reactions. Since, all the peaks recorded for DPPC liposomes in the present study via DSC were endothermic, then, no decomposition reactions were evident in DPPC liposomes due to encapsulation. The physicochemical characterization of liposomes, such as size, shape, and charge are vital parameters to deliver improved bio-distribution and prolonged pharmacokinetics of encapsulated cytotoxic drugs (Krasnici et al. 2003; Li et al. 2016).

Curcumin has a potency to defend a variety of cancers. Scientists are now seeking for new methods of drug loading to increase drug bioavailability, bio-distribution, targeting, and to get rid of the possible side effects of drugs and this is a growing strategy to treat proliferative diseases like neoplasms. Based on this concept, liposomal formulations of curcumin had shown increased cytotoxicity to cancer cells owning to their improved bioavailability.

Recent researchers demonstrated that curcumin is more toxic to cancer cells than normal cells. This fact was supported by the study of Deer et al. (2010) that showed that curcumin induces apoptosis through ROS in cancer cells but not in normal cells. This is mainly due to the ability of curcumin to bind more than 40 different proteins and to affect many cancer cell pathways; it can greatly affect the growth regulation of tumor cells through the effect it exerts on multiple cell-signaling pathways (Syng-ai et al. 2004; Ravindran et al. 2009). One known mechanism of the mechanism of action of curcumin on cancer cells is the activation of the NF-κB pathway and the

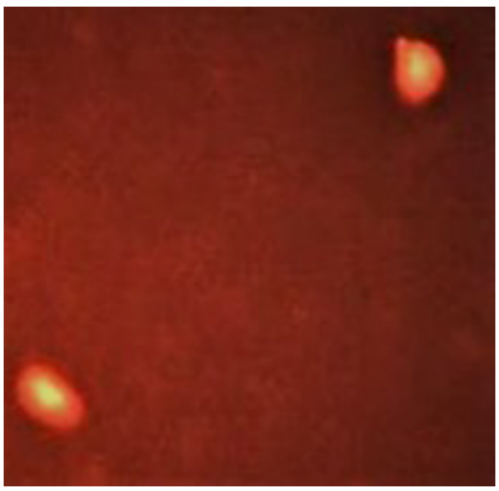

Fig. 8 Intact nuclei without damage or tail in untreated A549 lung cancer cells

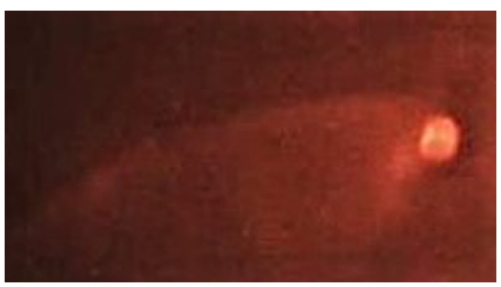

Fig. 9 Nuclei show a high degree of damage in A549 cells treated with thymoquinone, curcumin-encapsulated liposome

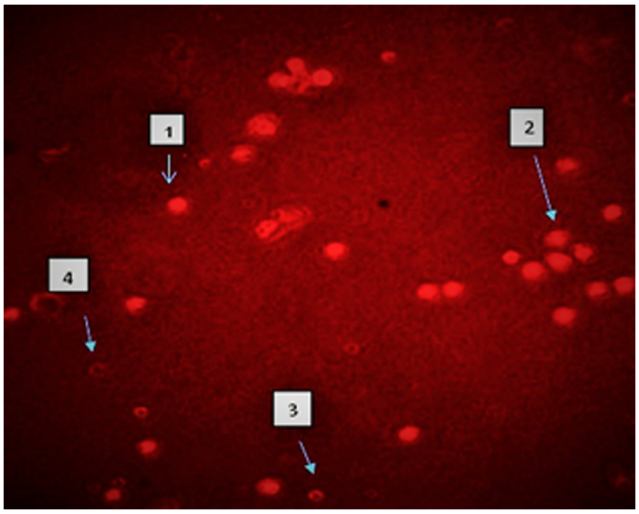

Fig. 10 A549 cells treated with thymoquinone, curcumin, and rhodamine B-encapsulated liposome under inverted fluorescence microscope. (1) Viable cells with normal nuclei, (2) viable cells with apoptotic nuclei, (3) dead cells with normal nuclei, and (4) dead cells with apoptotic nuclei

expression of various oncogenes regulated by NF-κB, which leads to cancer cell apoptosis (Lin et al. 2007).

Treatment of A549 lung cancer cells with the liposome formulation: thymoquinone + curcumin + rhodamine B-encapsulated DPPC liposome stops the proliferation of cancer cells, probably by enhancing cell uptake, through the generation of oxidative stress damage (as expressed by the significant increase in the levels of malondialdehyde: the result of the cell membrane peroxidation in addition to the significant decrease in the activity of the enzyme SOD which is a natural antioxidant found in the cells). This induced oxidative stress damage in the A549 lung cancer cells due to its treatment with thymoquinone + curcumin + rhodamine B-encapsulated DPPC liposome leads to DNA damage (as manifest from the comet assay results received from the present survey) and cell apoptosis (as shown by the micrographs obtained from the inverted fluorescence microscope).

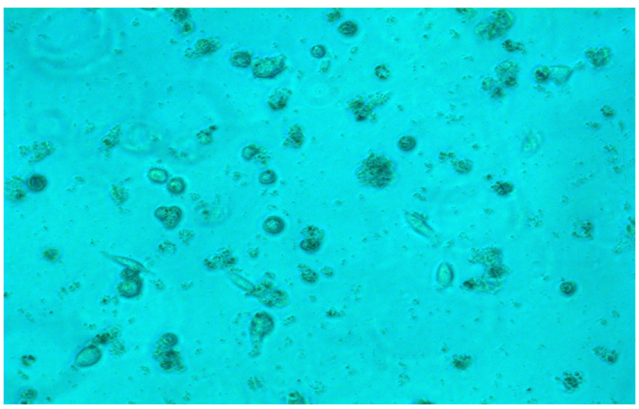

Fig. 11 Untreated A549 lung cancer cells under inverted fluorescence microscope

Conclusions

From the outcomes obtained in the present work, it may be concluded that the encapsulation of DPPC liposomes with thymoquinone and/or curcumin resulted in the modification of the physical properties of DPPC liposomes. Thymoquinone + curcumin + rhodamine B-encapsulated DPPC liposome is a promising cytotoxic agent for A549 lung cancer cells as it decreases the proliferation of cancer cells through the generation of oxidative stress damage which leads to DNA damage and cell apoptosis. When analyzed for its power to suppress the growth of cancer cells, thymoquinone + curcumin + rhodamine B-encapsulated DPPC liposome was more potent than either free curcumin or free TQ or the liposomal formulation of either of them, possibly due to enhanced uptake.

Further studies are still needed to optimize the dose used and to test this promising formulation on other cancer cell lines types and in vivo applications are still missing.

Acknowledgments The author would like to thank Sahar El Sayed Ahmed and Heba Ahmed Rashed for their help during the practical part of the work.

Author contribution statement HMF conceived and designed research, conducted experiments, analyzed data, and wrote the manuscript. HMF read and approved the manuscript.

Compliance with ethical standards

Conflict of interest The authors declare that there is no conflict of interest.

References

Aggarwal BB, Kumar A, Bharti AC (2013) Anticancer potential of curcumin: preclinical and clinical studies. Anticancer Res 23(1A): 363–398

Badary OA, Al-Shabanah OA, Nagi MN, Al-Bekairi AM, Elmazar MMA (1998) Acute and subchronic toxicity of thymoquinone in mice. Drug Dev Res 44:56–61

Bangham AD, Hill MW, Miller NGA (1974) Preparation and use of liposomes as models of biological membranes. Methods in Membrane Biology, vol 1. Plenum Press, New York, pp l–68

Beutler E, Duron O, Kelly BM (1963) Improved method for the determination of blood glutathione. J Lab Clin Med 61:882–888

Bozzuto G, Molinari A (2015) Liposomes as nanomedical devices. Int J Nanomedicine 10:975

Chauhan DP (2002) Chemotherapeutic potential of curcumin for colorectal cancer. Curr Pharm Des 8:1695–1706

Deer EL, Gonzalez-Hernandez J, Coursen JD, Shea JE, Ngatia J, Scaife CL et al (2010) Phenotype and genotype of pancreatic cancer cell lines. Pancreas. 39:425±435. https://doi.org/10.1097/MPA.0b013e3181c15963

Dehghani H, Hashemi M, Entezari M, Mohsenifar A (2015) The comparison of anticancer activity of thymoquinone and nanothymoquinone on human breast adenocarcinoma. Iranian journal of pharmaceutical research: Iran J Pharm RES 14(2):539–546

Díaz-Visurraga J, Daza C, Pozo C, Becerra A, von Plessing C, García A (2012) Study on antibacterial alginate-stabilized copper nanoparticles by FT-IR and 2D-IR correlation spectroscopy. Int J Nanomedicine 7:3597–3612

Farrow SN, Brown R (1996) New members of the Bcl-2 family and their protein partners. Curr Opin Genet Dev 6(1):45–49

Felice B, Prabhakaran MP, Rodríguez AP, Ramakrishna S (2014) Drug delivery vehicles on a nano-engineering perspective. Mater Sci Eng C Mater Biol Appl 41:178–195

Gali-Muhtasib H, Roessner A, Schneider-Stock R (2006) Thymoquinone: a promising anti-cancer drug from natural sources. Int J Biochem Cell Biol 38(8):1249–1253

Goel A, Boland CR, Chauhan DP (2001) Specific inhibition of cyclooxygenase-2 (COX-2) expression by dietary curcumin in HT-29 human colon cancer cells. Cancer Lett 172(2):111–118

Guo H, Xu YM, Ye ZQ, Yu JH, Hu XY (2013) Curcumin induces cell cycle arrest and apoptosis of prostate cancer cells by regulating the expression of IκBα, c-Jun and androgen receptor. Die Pharmazie - An International Journal of Pharmaceutical Sciences 68(6):431–434

Harris JM, Martin NE, Modi M (2001) Pegylation: a novel process for modifying pharmacokinetics. Clin Pharmacokinet 40:539–551

Heurtault B, Saulnier P, Pech B, Proust JE, Benoit JP (2003) Physico-chemical stability of colloidal lipid particles. Biomaterials. 24:4283–4300

Jacobs C, Müller RH (2002) Production and characterization of a budesonide nanosuspension for pulmonary administration. Pharm Res 19:189–194

Jin H, Qiao F, Wang Y, Xu Y, Shang Y (2015) Curcumin inhibits cell proliferation and induces apoptosis of human non-small cell lung cancer cells through the upregulation of miR-192-5p and suppression of PI3K/Akt signaling pathway. Oncol Rep 34(5):2782–2789

Karunagaran D, Rashmi R, Kumar TR (2005) Induction of apoptosis by curcumin and its implications for cancer therapy. Curr Cancer Drug Targets 5:117–129

Khan MA, Tania M, Fu S, Fu J (2017) Thymoquinone, as an anticancer molecule: from basic research to clinical investigation. Oncotarget. 8(31):51907

Krasnici S, Werner A, Eichhorn ME, Schmitt-Sody M, Pahernik SA, Sauer B, Schulze B, Teifel M, Michaelis U, Naujoks K, Dellian M (2003) Effect of the surface charge of liposomes on their uptake by angiogenic tumor vessels. Int J Cancer 105:561±567–561±567. https://doi.org/10.1002/ijc.11108

Kurzrock R, Li L (2005) Liposome-encapsulated curcumin: in vitro and in vivo effects on proliferation, apoptosis, signaling, and angiogenesis. J Clin Oncol 23:4091

Lasic DD (1998) Novel applications of liposomes. Trends Biotechnol 16: 307–321

Li L, Xiang D, Shigdar S, Yang W, Li Q, Lin J, Liu K, Duan W (2014) Epithelial cell adhesion molecule aptamer functionalized PLGA-lecithin-curcumin-PEG nanoparticles for targeted drug delivery to human colorectal adenocarcinoma cells. Int J Nanomedicine 9:1083

Li H-J, Du J-Z, Du X-J, Xu C-F, Sun C-Y, Wang H-X, et al. (2016) Stimuli-responsive clustered .33 nanoparticles for improved tumor penetration and therapeutic efficacy. Proc Natl Acad Sci, Early Edit: 201522080

Lin YG, Kunnumakkara AB, Nair A, Merritt WM, Han LY, Armaiz-Pena GN et al (2007) Curcumin inhibits tumor growth and angiogenesis in ovarian carcinoma by targeting the nuclear factor-kappa B pathway. Clin Cancer Res 13:3423±3430. https://doi.org/10.1158/1078-0432.CCR-06-3072

Lin SS, Lai KC, Hsu SC, Yang JS, Kuo CL, Lin JP, Ma YS, Wu CC, Chung JG (2009) Curcumin inhibits the migration and invasion of human A549 lung cancer cells through the inhibition of matrix metalloproteinase-2 and-9 and vascular endothelial growth factor (VEGF). Cancer Lett 285(2):127

Ma J, Fang B, Zeng F, Pang H, Zhang J, Shi Y, Wu X, Cheng L, Ma C, Xia J, Wang Z (2014) Curcumin inhibits cell growth and invasion through up-regulation of miR-7 in pancreatic cancer cells. Toxicol Lett 231(1):82–91

Majdalawieh AF, Fayyad MW, Nasrallah GK (2017) Anti-cancer properties and mechanisms of action of thymoquinone, the major active ingredient of Nigella sativa. Crit Rev Food Sci Nutr 57(18):3911–3928

Makino K, Yamada T, Kimura M, Oka T, Ohshima H, Kondo T (1991) Temperature-and ionic strength-induced conformational changes in the lipid head group region of liposomes as suggested by zeta potential data. Biophys Chem 41:75–183

Mishra PR, Alshaal L, Muller RH, Keck CM (2009) Production and characterization of Hesperetin nanosuspensions for dermal delivery. International journal of pharmaceutics. 371(1-2):182–189

Nishikimi M, Roa NA, Yogi K (1972) The occurrence of superoxide anion in the reaction of reduced phenazine methosulfate and molecular oxygen. Biochem bioph res commun 46:849–854

Oetari S, Sudibyo M, Commandeur JN, Samhoedi R, Vermeulen NP (1996) Effects of curcumin on cytochrome P450 and glutathione S-transferase activities in rat liver. Biochem Pharmacol 51:39–45

Patil S, Sandberg A, Heckert E, Self W, Seal S (2007) Protein adsorption and cellular uptake of cerium oxide nanoparticles as a function of zeta potential. Biomaterials. 28:4600–4607

Randhawa MA, Alghamdi MS (2011) Anticancer activity of nigella sativa (black seed): a review. Am J Chin Med 39:1075–1091

Ravindran J, Prasad S, Aggarwal BB (2009) Curcumin and cancer cells: how many ways can curry kill tumor cells selectively? AAPS J 11: 495±510–495±510. https://doi.org/10.1208/s12248-009-9128-x

Ravindran J, Nair HB, Sung B, Prasad S, Tekmal RR, Aggarwal BB (2010) Thymoquinone poly (lactide-co-glycolide) nanoparticles exhibit enhanced antiproliferative, anti-inflammatory, and chemosensitization potential. Biochem Pharmacol 79:1640–1647

Ruiz-Larrea MB, Leal AM, Liza M, Lacort M, de Groot H (1994) Antioxidant effects of estradiol and 2-hydroxyestradiol on ironinduced lipid peroxidation of rat liver microsomes. Steroids: 59, 383–388 17

Shameli, K.; Bin Ahmad, M.; Jazayeri, S. D.; Shabanzadeh, P Jahangirian, H.; Mahdavi, M.; Abdullahi, (2012): Synthesis and characterization of polyethylene glycol mediated silver nanoparticles by the green method

Shehzad A, Lee J, Huh TL, Lee YS (2013) Curcumin induces apoptosis in human colorectal carcinoma (HCT-15) cells by regulating expression of Prp4 and p53. Molecules and cells 35(6):526–532 Y Int J Mol Sci 13, 6639–6650

Srivastava RK, Chen Q, Siddiqui I, Sarva K, Shankar S (2007) Linkage of curcumin-induced cell cycle arrest and apoptosis by cyclin dependent kinase inhibitor p21 (/WAF1/CIP1). Cell Cycle 6:2953–2961

Svarnas P, Matrali SH, Gazeli K, Aleiferis S, Clément F, Antimisiaris SG (2012) Atmospheric-pressure guided streamers for liposomal membrane disruption. Appl Phys Lett 101:264103

Syng-ai C, Kumari AL, Khar A, Syng-ai C, Kumari AL (2004) Effect of curcumin on normal and tumor cells: Role of glutathione and bcl-2 Effect of curcumin on normal and tumor cells: Role of glutathione and bcl- 2; 3: 1101±1108

Thangapazham RL, Sharma A, Maheshwari RK (2006) Multiple molecular targets in cancer chemoprevention by curcumin. AAPS J 8: E443–E449

Toyran N, Severcan F (2002) Infrared spectroscopic studies on the dipalmitoyl phosphatidylcholine bilayer interactions with calcium phosphate: effect of vitamin D 2. J Spectrosc 16:399–408

Wilken R, Veena MS, Wang MB, Srivatsan ES (2011) Curcumin: a review of anti-cancer properties and therapeutic activity in head and neck squamous cell carcinoma. Mol Cancer 10(1):12

Wong KE, Ngai SC, Chan KG, Lee LH, Goh BH, Chuah LH (2019) Curcumin nanoformulations for colorectal cancer: a review. Front Pharmacol ;10

Worthen DR, Ghosheh OA, Crooks PA (1998) The in vitro anti-tumor activity of some crude and purified components of black seed Nigella sativa L. Anticancer Res 18:1527–1532

Yang J, Kuang XR, Lv PT, Yan XX (2015) Thymoquinone inhibits proliferation and invasion of human nonsmall-cell lung cancer cells via ERK pathway. Tumor Biol 36(1):259–269

Zamboni WC (2008) Concept and clinical evaluation of carrier mediated anticancer agents. Oncologist. 13:248–260

Zhen L, Fan D, Yi X, Cao X, Chen D, Wang L (2014) Curcumin inhibits oral squamous cell carcinoma proliferation and invasion via EGFR signaling pathways. Int J Clin Exp Pathol 7:6438–6446